Strojniški vestnik - Journal of Mechanical Engineering 70(2024)7-8, 392-402
DOI:10.5545/sv-jme.2024.921
Original Scientific Paper
Received for review: 2024-01-10
Received revised form: 2024-05-02
Accepted for publication: 2024-05-30

The Use of Heuristic Optimization Techniques on RV Cycloid Reducer Design: A Comparative Study

Furkan Korkmaz[1,*] – Serkan Dereli[1] – Durmuş Karayel[2] – Ahmet Kolip[2]
[1]Sakarya University of Applied Sciences, Sakarya Vocational School, Turkey
[2]Sakarya University of Applied Science, Technology Faculty, Turkey

In this study, heuristic optimization algorithms such as particle swarm optimization (PSO) and quantum particle swarm optimization (QPSO) have been used to optimize the weight of the cycloid reducer based on the values of some parameters. The algorithms were applied separately to the design problem, and their performances were compared. Initially, a basic design was performed using conventional approaches. Constraint conditions have been defined based on geometric features and the essential component of the reducer, the cycloidal gear, and then the existing basic design has been optimized in terms of size and weight. Finally, finite element analysis was conducted to validate the obtained parameter values and control the stresses in the contact areas of the cycloid gear profile. It has been determined that PSO reduced the weight of the basic design by 33.3 %, whereas QPSO reduced it by 33.8 %. Moreover, the results of the finite element analysis showed that the design obtained according to both optimization methods was safe in terms of the resulting stresses. Consequently, it has been demonstrated that the selected design parameters and constraint equations have been sufficient and that the basic designs could be enhanced using intuitive optimization methods.

Keywords: cycloid reducer, finite element analysis, optimization, heuristic algorithm

Highlights

- *The research provides comprehensive constraint conditions necessary to reduce the weight of cycloidal reducers.*
- *It shows that PSO and QPSO algorithms are suitable optimization methods for cycloidal reducers.*
- *It shows that optimization methods are an accurate method for improving uncertain design parameters.*
- *It recommends the control of cycloidal reducers by finite element analysis after optimization.*

0 INTRODUCTION

Cycloid reducers are important as a power transmission mechanism in sectors requiring high precision. They are characterized by their high efficiency, low noise, and compact size. Cycloid reducers are generally used in a variety of applications, including machine tools, robotics, and wind turbines. Studies on cycloidal reducers have increased, especially with advances in robotic technology, focusing on analytical definitions for profile modification, geometry verification by numerical analysis, and optimization studies. Several researchers have proposed innovative methods for profile modification in cycloid reducers, such as optimizing the tooth shape to improve performance and reduce backlash. Some publications dealing with the profile equation suggested a new profile equation due to the complexity of the modification equation and the inability to improve the obtained result **[1]** and **[2]**. In the study of Li et al. **[2]**, taking into account the pressure angle distribution characteristics, meshing backlash, tooth tip, and tooth root clearances, the modified profile is obtained by shifting the theoretical tooth profile in the direction of the normal contact point. Xu et al. **[3]** examined the effect of design parameters on load distribution and contact stresses. When creating profile equations, gaps and assembly errors must also be taken into account **[4]** to **[7]**. Yang et al. **[4]** developed the mathematical model of the closed-loop mechanism of the cycloid reducer. Manufacturing and assembly errors were added to the analytical model, and their effects were examined. Korkmaz and Karayel **[8]** studied on a prestressed system to prevent clearance between the cycloid gear and the pin. Another important criterion for profile design is the characteristic of the load distribution. It is expected that the load will be distributed on half of the pins and will change curvilinearly **[9]** to **[11]**. Li et al. **[10]** investigated the effects of radial and angular defects in ring pins on load distribution and maximum contact stress.

Numerous researchers used numerical analysis techniques to evaluate and optimize key parameters such as contact stress, efficiency, backlash, and dynamic behaviour to achieve optimal performance in cycloid reducers. Matejic et al. **[12]** observed the internal stresses on the cycloid gears, which is the most important element of cycloid reducers. For this purpose, they made a finite element analysis of the model they created and compared it with the experimental results. It was emphasized that the experimental and simulation results were quite close as an important condition in the results obtained. Also, this situation shows that it is appropriate to use

*Corr. Author's Address: Sakarya University of Applied Sciences, Sakarya Vocational School, Turkey, fkorkmaz@subu.edu.tr

simulations in cycloid reducers. Jiang et al. used the finite element analysis method to verify the effect of the profile equation they created on the load distribution characteristic [1].

Optimization techniques were widely used in the field of cycloid reducer design to enhance their performance and efficiency [13] to [15]. Zhang et al. [16] conducted an optimization study on the carrying capacity of crank bearings in rotate vector (RV) reducers. In the study, a multi-objective genetic algorithm was used, and the results were confirmed by finite element analysis. Wang et al. [17] also proposed a methodology to maximize efficiency while minimizing the volume of the reducer using a genetic algorithm. Zhang et al. [18] determined three objective functions: high tensile, high efficiency, and low lightness parameters and thirteen boundary conditions. They used the non-dominated searching genetic algorithm (NSGA-II) as the optimization method. In the results, it was stated that as a result of the optimization, efficiency was increased, the weight was reduced, and the design parameters were provided. Huang et al. [19] focused on a more specific area. In their work, they carried out an optimization study to improve the profile of the bearings and crowned roller profile. The Crow Search Algorithm (CSA) was used, and it was stated that the bearing life increased in the results obtained.

Optimization is crucial in the design of cycloidal reducers, as in other types of reducers. Cycloidal reducers are generally optimized for efficiency, durability, size and weight, cost, vibration, and noise control. Size and weight significantly impact other variables that need optimization in the design of these reducers. Indeed, the optimization of size and weight plays a vital role in meeting performance, efficiency, economic, and overall system requirements in reducer design. Therefore, this study focuses on weight optimization.

Changes in the design parameters of the cycloidal gear, the fundamental component of cycloidal reducers, directly affect the dimensions of other parts of the reducer. Simultaneously, alterations in the design parameters lead to a change in the profile. The strength and performance characteristics of cycloidal reducers are determined by the cycloidal gear profile. Considering existing literature studies, it has been decided to optimize the determined design parameters by accurately defining constraint equations, aiming to minimize weight.

Reviewing optimization studies on cycloidal reducers, it is observed that, typically, reliance is placed on a single algorithm. However, it is evident from the literature that different optimization algorithms yield different results for the same objective. Certain algorithms demonstrate superior performance under specific conditions, while others might not deliver the same level of effectiveness. This is attributed to the fact that optimization algorithms might perform better for certain types of problems or conditions. The initial effectiveness of an algorithm on a particular problem is not always apparent. Despite the use of multiple algorithms in the literature, particle swarm optimization (PSO) stands out due to its ease of application, broad applicability, parallel processing capability, less parameter sensitivity, rapid convergence, and flexible parameter adjustment. Hence, in this study, the PSO and a version based on quantum mechanics principles, namely quantum particle swarm optimization (QPSO), have been utilized. Subsequently, three different designs obtained through the PSO, QPSO algorithms, and a general design approach have been compared against each other.

The designs obtained from both optimization algorithms have clearly shown better results in terms of weight compared to the basic design, as explicitly observed in the Result and Discussion section. Comparing the performance of two different algorithms and demonstrating the suitability of the optimization for the problem stands out as an originality of this study. For each optimization result, a new design has been executed, analysed, and compared with the basic design. Consequently, besides validating the optimization algorithm, factors not explicitly defined as constraints in the optimization, such as stresses, have been reviewed. This can be put forth as another differentiation of this study from other research in the field.

1 CYCLOID REDUCER DESIGN AND PARAMETERS

The profile of the cycloid gear, which is the most important part of cycloid reducers, varies according to the eccentricity (e), the diameter of the pins' locating circle (D_z), and the diameter of the pins (d_z). Design variables in cycloid gears also affect other equipment in the gearbox geometrically. Because of this situation, it directly affects the weight of the reducer and the efficiency of the system.

1.1 Geometry of Cycloid Reducer

RV cycloidal reducers have two stages: planetary and cycloidal. The first stage involves a planetary mechanism (Fig. 1 (1)), which offers several

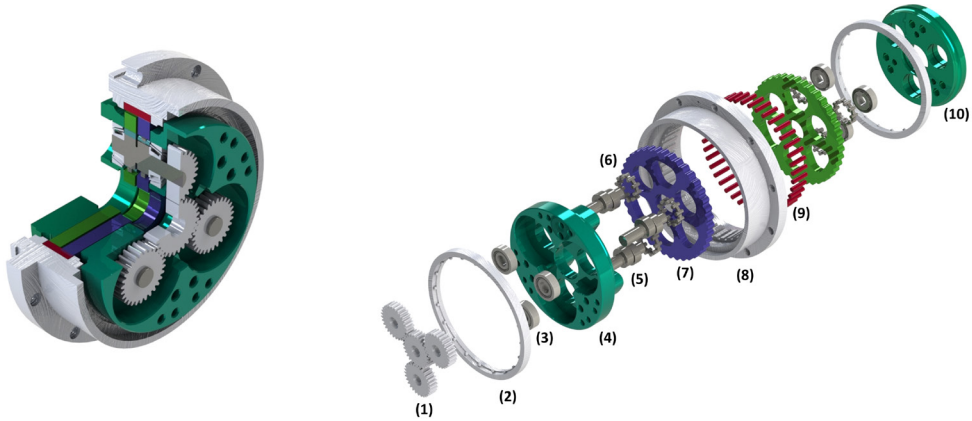

Fig. 1. *RV Cycloid reducer structure; (1) planet, (2) main bearing, (3) angular bearing, (4) front cover, (5) crank, (6) crank bearing, (7) cycloid gear, (8) case, (9) pins, and (10) rear cover*

significant advantages. Firstly, the planetary mechanism directly influences the transmission ratio, allowing for precise control of the output speed. Secondly, it efficiently distributes the torque from the input shaft to the cranks (Fig. 1 (5)), which then transfers the torque to the second stage, ensuring smooth and reliable power transmission. It consists of the cycloid gear(s) (Fig. 1 (7)), which is the key part of the second stage reducer of cycloid reducers. In this study, the geometry of the cycloid gear has been optimized, especially considering the contact stresses and weight. The exploded view of the cycloid reducer and assembly used in the study is given in Fig. 1.

2 OPTIMIZATION TECHNIQUES

Nowadays, optimization methods are frequently used by researchers to solve complex and non-linear problems. Because classical numerical methods approach problems in a certain way, they produce very unsuccessful results in obtaining the optimum value of the problem [20]. For this reason, heuristic techniques inspired by the behaviour of creatures in nature have become very popular among researchers. The fact that they can produce a large number of optimum values, especially in many systems with multiple parameters, has further increased the fame of these techniques [21]. These techniques have been able to produce effective solutions to problems in many different fields within mechanical engineering with a single fitness function [22]. In one study, a new method was proposed based on the wolf algorithm, which is considered an up-to-date heuristic algorithm, in order to estimate the rotation error of the RV reducer in the most accurate and fastest way [23]. In their work, they used seven different up-to-date heuristic algorithms to achieve the design of a two-stage gearbox with optimum values in terms of volume [24]. In this study, a cycloid reducer design with the most optimum values in terms of weight and size has been performed. The optimum values of the variables of the gear have been obtained separately with both standard PSO and quantum PSO techniques and compared in terms of results.

Classical PSO is an algorithm that has been widely studied in the literature, is accepted as the starting algorithm of heuristic techniques, and can be easily applied to the problem due to the small number of control parameters. Therefore, it is an important algorithm whose usability and ability to produce solutions to problems have been proven many times [25]. The PSO algorithm, which shows the power of the swarm effect in reaching a solution by a swarm of birds or fish moving together while reaching a target, is depicted in Fig. 2 in terms of the movement of the particles [26]. As can be clearly seen from this figure, all of the particles are moving towards the target at a certain speed:

1. Randomly initial values in the appropriate range
2. Loop iteration
3. Loop particles
4. Calculate the fitness function (According to Section 2.2)
5. Find the value of *Pbest*
6. Update particle velocity value
7. Update particle position
8. Detection of constraint situations (According to Section 2.3)
9. End particle loop
10. Find the value of *Gbest*
11. End iteration loop
12. Return *Gbest* value

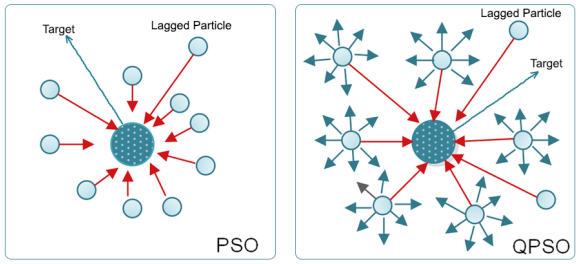

Fig. 2. *Movements of particles in standard PSO and quantum PSO techniques*

As seen in the pseudo-code expressing the flow of the particle swarm algorithm above, the only parameter in the algorithm is the velocity value calculated in line 6. Since this value is the particle's approach parameter to the target, it is recalculated for each particle in each iteration. Therefore, the particles approach the target at a certain distance based on *Pbest* and *Gbest* values. In this flow, the only step that changes from problem to problem is the line where the fitness function calculation is made in step four. Other steps remain largely the same.

The Quantum PSO technique, which is similar in name to the classical PSO algorithm, has come to the fore because the particles have a more dynamic structure, bypassing local convergence situations and guaranteeing the global optimum value [27]. In fact, Fig. 2 clearly depicts the movement of particles in both PSO and Quantum PSO algorithms. According to this figure, it is clear that all particles in the PSO algorithm are moving in the same direction. This situation is the biggest obstacle to a particle that is already lagging behind in reaching the optimum value and causes the algorithm to frequently get stuck at the local optimum value [28]. In Quantum PSO, inspired by quantum wavelet motion, all particles have the ability to move in any direction, according to this figure. Therefore, a particle lagging behind can easily reach the optimum value. This prevents the algorithm from being stuck in local best values and ensures that it obtains the global best value [29].

1. Randomly initial values in the appropriate range
2. Loop iteration
3. Compute *MBest* (Average of *Pbest* Particles)
4. Loop particles
5. Calculate the fitness function
6. Calculate quantum wavelength
7. Update particle position
8. Detection of constraint situations (According to Section 2.3)
9. End particle loop
10. End iteration loop
11. Return *Gbest* value

As seen in the pseudo-code of the Quantum PSO algorithm above, wavelength theory and the average of local best values are used for the next position of the particle. Of course, as in all stochastic algorithms, randomness is very important in heuristic algorithms that search in a certain solution space. In both the standard PSO algorithm and the Quantum PSO algorithm, this is effective in determining the new position of the particles. However, it is clearly seen in the literature that this alone is not sufficient in terms of the PSO algorithm [30].

In this study, the minimization of the weight and dimensions of a cycloidal reducer has been considered as an optimization problem. The objective functions, design variables, and constraints defined for the optimization problem are provided below.

2.1 Design Variables

One of the most important parameters for reducers is the transmission ratio. This ratio is calculated according to the relative transmission ratio formula for RV reducers. The relative transmission ratio formula for the RV reducer is as follows. [31] and [32]:

$$i = \frac{1}{1+\frac{z_3}{z_4}z_2}, \tag{1}$$

here, z_3 and z_4 are the tooth numbers of the sun gear and planet gear, respectively. They are taken equally because of the focus on the cycloid disk geometry. The reducer transmission ratio was preferred to be 1/40. For this reason, the number of lobes in the disks (z_1) is 39, and the number of pins (z_2) is 40.

A new geometry has been designed considering the design parameters in Table 1 for the sample application. The parameters were decided according to the 1/40 transmission ratio.

The eccentricity (e), the diameter of the pins' locating circle (D_z), the diameter of the pins (d_z) and the thickness of the cycloid gear (B) have been accepted as the design parameters. These parameters also affect the geometry of other parts that make up the gearbox:

$$\mathbf{X} = [e, D_z, d_z, B]. \tag{2}$$

The lower and upper limits of the optimization parameters given in Table 1 were chosen close to the values in articles and catalogues containing previous successful application examples. Thus, it is aimed to protect against possible risks that may arise in the material supply, manufacturing, assembly and operating performance of the reducer parts.

Table 1. *Design variables and values for cycloid reducer*

Parameter	Symbol, unit	Initial value	Upper and lower limits
Eccentricity	e [mm]	1.5	$0.8 \le e \le 2$
Diameter of the pins' locating circle	D_z [mm]	154	$110 \le D_z \le 160$
Pin diameter	d_z [mm]	6	$4 \le d_z \le 8$
Thickness of cycloid gear	B [mm]	11	$6.4 \le B \le 12.8$

2.2 Objective Function

When calculating the weights of the cycloid gears, which form the main part of the reducer, the cycloid gear e, D_z, d_z, B profile and the spaces inside are taken into account. The main dimensions of the cycloid gear are determined by other parts that make up the crank and front-rear cover fastening spaces. For this reason, when calculating the cycloid gear weight, the weights of other parts are usually included in the objective function of the optimisation study. These parts are cycloid gear (G_1), case (G_2), crank (G_3) and pin (G_4). Also, we defined some coefficients in the objective function. We have 2 cycloid gears, 4 same-size planet gears, 3 cranks and 40 pins:

$$G = 2\times G_1 + G_2 + 3\times G_3 + 40\times G_4. \tag{3}$$

2.2.1 Weight of Cycloid Gear

When calculating the weight of the cycloid gear, internal spaces are subtracted from the mean disc diameter (D_b). These spaces are the spaces opened for the input shaft (D_s), cranks (D_u) and front-rear cover connections (D_k). These terms are given in Fig. 3.

$$G_1 = B\rho\left[\left(\int_{r=0}^{2\pi}\int_{\beta=0}^{\sqrt{x_c^2+y_c^2}} r\,dr\,d\beta\right) - \frac{\pi}{4}\left(D_s^2 - z_k D_u^2 - 3D_k^2\right)\right], \tag{4}$$

where $K_1 = \dfrac{e\times z_2}{D_z/2}$, and

$S = \sqrt{1 + K_1^2 - 2\times K_1 \times \cos(z_1\varphi)}$ is the meshing phase angle. The x_c and y_c are the coordinates for meshing the points where the pin and the disk come into contact. The x_c and y_c coordinates are expressed as in Eq. (5):

$$\begin{cases} x_c = \dfrac{d_z}{2}\times\dfrac{K_1\sin(z_1\varphi)}{S} \\ y_c = \dfrac{D_z}{2} - \dfrac{d_z}{2}\times\dfrac{(1 - K_1\cos(z_1\varphi))}{S} \end{cases}, \tag{5}$$

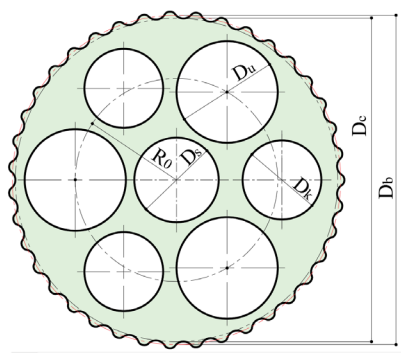

Fig. 3. *Cycloid gear parameters*

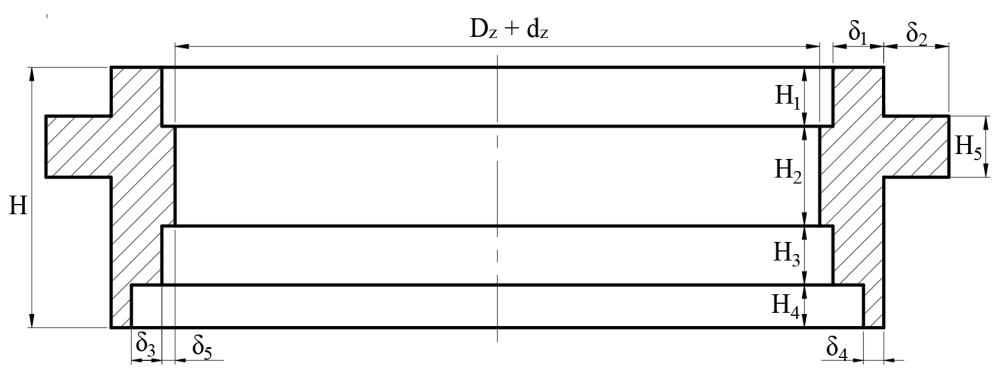

Fig. 4. *Case parameters*

$$G_2 = \frac{\pi}{4}\left\{\begin{array}{c}\left(D_z + 2\delta_1 + 2\delta_3\right)^2 H - \left[\left(D_z + 2\delta_3\right)^2 H_1 + (D_z^2 + 40\times d_z^2)H_2 + \left(D_z + 2\delta_3\right)^2 H_3 + \left(D_z + 2\delta_3 + 2\delta_5\right)^2 H_4\right] \\ + \left[\left(D_z + 2\delta_1 + 2\delta_2 + 2\delta_3\right)^2 - \left(D_z + 2\delta_1 + 2\delta_3\right)^2\right] H_5\end{array}\right\} \times \rho_c. \tag{6}$$

2.2.2 Weight of Case

The case varies according to the cycloid gear dimensions. Parameters of the case are given in Fig. 4.

2.2.3 Weight of Crank

The dimensions of the cranks vary according to the cycloid gear geometry and the torque value expected from the system.

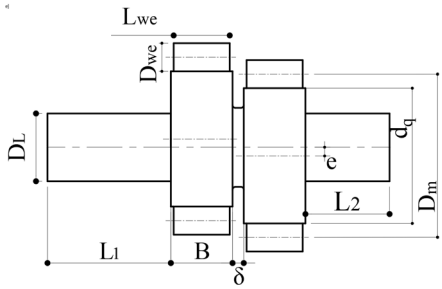

Fig. 5. *Cranks parameters*

$$G_3 = \frac{\pi}{4}\left[d_q^2 \left(2 \times B\right) + D_L^2 (L_1 + L_2) \right] \rho_{cr}. \tag{7}$$

2.2.4 Weight of Pins

The diameters of the pins (d_z) directly affect the cycloid gear profile. In addition, the lengths of the pins (l) are usually 0.5 mm more than the cycloid gear's thickness.

$$G_4 = \frac{\pi}{4} d_z^2 l \rho_{pin}. \tag{8}$$

2.3 Constraint Conditions

In optimization applications, accurate constraint conditions must be identified, and boundaries should be framed to ensure reliable results. To achieve this, constraint conditions commonly used in the literature have been evaluated and adapted for our specific problem.

2.3.1 Bearing Clearances in the Cycloid Gear

The outer raceway ($D_m + D_{we}$) is situated between the root circle (D_c) and the central hole (D_s) of the cycloidal gear. Consequently, the bearing pitch diameter must be less than the gap between the diameter of the central hole and the diameter of the root circle. However, the diameters (D_L) of the sections of the cranks mounted with the planet are related to the crank diameters and eccentricity [19]:

$$\begin{cases} g_1(x) = \left(D_m + D_{we}\right) - \dfrac{D_c - D_s}{2} < 0 \\ g_2(x) = D_L - \left(D_m - D_{we} + 2e\right) < 0 \end{cases}. \tag{9}$$

2.3.2 Distance Between Clearances

Another important constraint for RV reducers is the thickness of the outer ring of the eccentric bearings. Although the eccentric bearings used in RV reducers do not use an outer ring, the gap between the crank clearance and the tooth root diameter, as well as the gap between the crank clearance and the centre hole. Therefore, the distance between the clearances on the cycloid gear must not be less than the required thickness of the outer ring. The required thickness of the outer ring is obtained by multiplying the roller diameter by the ring thickness coefficient (ε) [19] and [33]:

$$\begin{cases} g_3(x) = \dfrac{D_m + D_{we}}{2} + \dfrac{D_s}{2} + \varepsilon D_{we} - R_0 < 0 \\ g_4(x) = \dfrac{D_m + D_{we}}{2} + R_0 + \varepsilon D_{we} - \dfrac{D_c}{2} < 0 \end{cases}. \tag{10}$$

Here, R_0 is the radius of the distribution circle of the cranks relative to the centre of the cycloidal gear. The ring thickness coefficient varies between 0.3 and 0.5. In our problem, we have taken the value of 0.4 [19] and [34].

2.3.3 Bearing Rollers

In addition to the crank and cycloid gear dimensions, the dimensions of the bearing rollers located between the cycloid gear and the crank are also very important for the life of the reducer. Therefore, a general approach regarding the bearing rollers has been taken into consideration [19]:

$$g_5(x) = L_{we} - B < 0, \tag{11}$$

where L_{we} is the length of the bearing roller.

2.3.4 Width of Cycloid Gear

The width of the cycloid gear directly influences not only the structure of the body and the length of the

pins but also surface stresses. Therefore, it is of great importance [17].

2.3.5 Tooth Profile Structure

In addition to the damage that may arise from the surface hardness of the tooth profile, the fractures that may occur at the tooth root due to the profile structure should not be overlooked. When forming the tooth profile, the structure of the profile should be constrained with the given constraint below [14]:

$$g_8(x) = \frac{d_z}{D_z} - \frac{(1+K_1)^2}{1+K_1+Z_1K_1} \leq 0. \quad (13)$$

2.3.6 Modification Coefficient for Cycloid Gear

The modification coefficient leads to different profiles in cycloid gear. Therefore, it directly affects the contact stresses occurring in the cycloid gear [17]:

$$\begin{cases} g_9(x) = 0.65 - K_1 < 0 \\ g_{10}(x) = K_1 - 0.9 < 0 \end{cases}. \quad (14)$$

2.3.7 *Diameter of the Pins' Locating Circle*

The diameter of the reference circle where the pins are placed directly affects the dimensions of the body, crank, and cycloidal gear, as well as their profiles [16]:

$$\begin{cases} g_{11}(x) = 1.7\sqrt[3]{T_{in}} - D_z \leq 0 \\ g_{12}(x) = D_z - 2.6\sqrt[3]{T_{in}} \leq 0 \end{cases}. \quad (15)$$

2.3.8 *Contact Strength Between Cycloid Gear and Pin*

The most critical areas in cycloidal reducers are where pin-cycloid gear contact occurs. Therefore, during optimization processes, contact stresses between the pins and the cycloid gear must be specified as constraint conditions. Eq. (16) is defined for the constraint condition of the pin-cycloid gear contact stress [17]:

$$g_{13}(x) = 0.418\sqrt{\frac{E_e}{B\times\rho_{e_{\min}}}\times\frac{4.4T_{out}}{K1\times z_1\times Dz}} - \sigma_{HP} \leq 0. \quad (16)$$

The curvature radius ($\rho_{e_{\min}}$) is calculated by the following two equations [35]:

$$\rho_{e_{\min}} = \left|\frac{\rho_i \times d_z/2}{\rho_i - d_z/2}\right|. \quad (17)$$

The material selected for both the pin and the cycloid gear is 20MnCr5 (1.7147). Heat treatments are applied to harden the surface of cycloid gears. Because of that, the maximum allowable contact stress (σ_{HP}) value is more than the other steels. The mechanical properties are given in Table 2 [36].

Table 2. *Mechanical properties of 20MnCr5*

Maximum allowable contact stress, σ_{HP} [MPa]	Equivalent elastic modulus, E_e [MPa]	Yield strength [MPa]
1200	210000	700

3 RESULTS AND DISCUSSIONS

The design parameters obtained through PSO and QPSO algorithms, along with the rounded values of the optimization results, are provided in Table 3.

Table 3. *Initial value and PSO-QPSO algorithms rounding results*

Parameter	Initial value	PSO rounding results	QPSO rounding results	Upper and lower limits
Eccentricity	1.5	1.1	1.25	$0.8 \leq e \leq 2$
Diameter of the pins' locating circle	154	110.6	135.3	$110 \leq D_z \leq 160$
Pin diameter	6	4.2	6.3	$4 \leq d_z \leq 8$
Thickness of cycloid gear	11	11	11.7	$6.4 \leq B \leq 12.8$

The total weights obtained from the optimization studies conducted using PSO and QPSO algorithms are presented in Fig. 6. As observed in Fig. 6, the goal of achieving approximately a fifty percent reduction in weight compared to the basic design has been accomplished using QPSO.

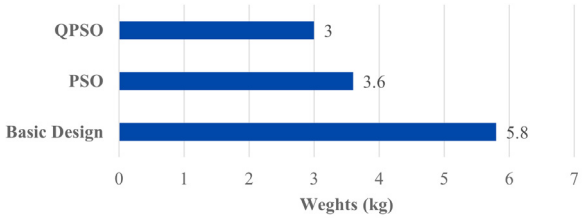

Fig. 6. *Total weight comparison of designs*

As seen in Fig. 7, the loads are distributed across half of the pins, taking the pin in the full grip position between the pins and the cycloid gear as the starting point. In the case of full engagement, the mechanism is theoretically assumed to have no

backlash and calculations are made according to the full engagement of the pins.

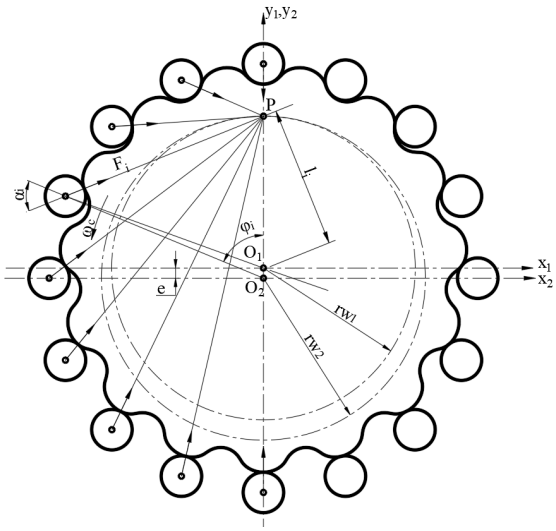

Fig. 7. *Load distribution on cycloid gear-pins*

As seen in Fig. 7, the virtual centroid circle with a radius of r_{w1} for the cycloid gear and the virtual centroid circle with a radius of r_{w2} for the pins are always tangent at a single point. φ_i indicates the angular position of each pin relative to the reference y-axis. The normal contact points of all pin-cycloid gears converge at this tangent point. Contact forces at the pin-cycloid gear contact points are calculated according to Eq. (18). The maximum meshing force ($F_{\max}$) occurs at the pin-cycloid gear contact point where the force arm (l_i) is maximum ($l_{\max} = r_{w1}$) **[37]**:

$$F_i = \frac{l_i}{r_{w1}} F_{\max}. \tag{18}$$

Generally, in RV cycloidal reducers that operate with two cycloid gears, the torque value cannot be evenly distributed due to manufacturing errors. Therefore, in the approach found in the literature, calculations are performed considering that 55 % of the output torque (T_{out}) is applied to one cycloid gear as if it were acting on the precision cycloid gear. In this study, the output torque value was taken as 300000 Nmm. Consequently, the maximum contact force is calculated according to Eq. (19) **[37]**:

$$F_{\max} = \frac{4 \times 0.55 \times T_{out}}{e \times z_1 \times z_2}. \tag{19}$$

Eq. (20) is used when calculating the contact forces at the contact points separately for each pin ($i = 1, 2, \ldots, 40$):

$$F_i = \frac{F_{\max} \cdot (D_z / 2) \times \sin\varphi}{\sqrt{\frac{D_z^2}{4} + (z_2 \times e)^2 - D_z \times z_2 \times e \cdot \cos\varphi}}. \tag{20}$$

Eq. (20) has been used to calculate the load distributions for three designs based on the values in Table 3. The resulting load distributions are given comparatively in Fig. 8 as basic design, PSO and QPSO. When examining the load distribution under a torque of 300000 Nmm, it is observed that the design with the highest maximum load occurs in the QPSO, which also has the lowest weight among the designs. Additionally, another observation in the load distribution is that the distribution between the pins is more regular in the basic design compared to PSO and

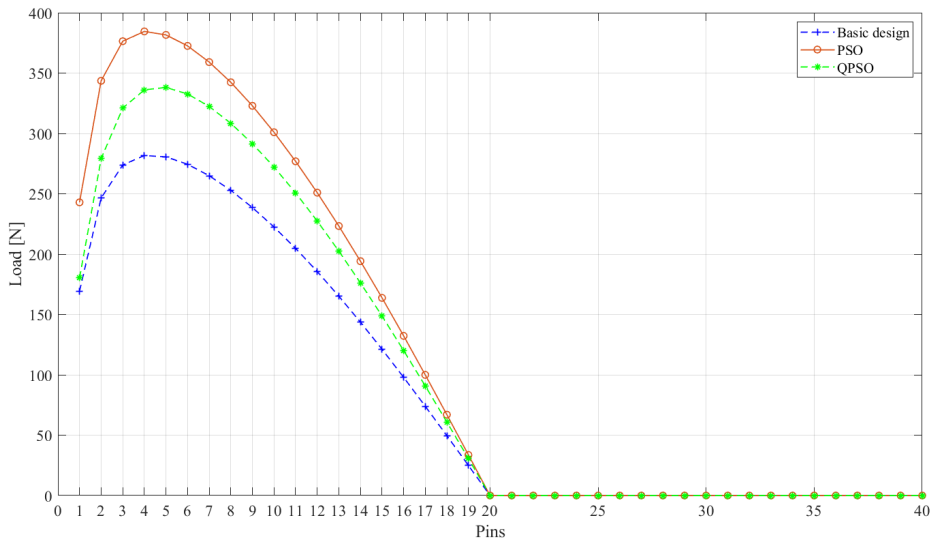

Fig. 8. *Comparative load distribution graphs*

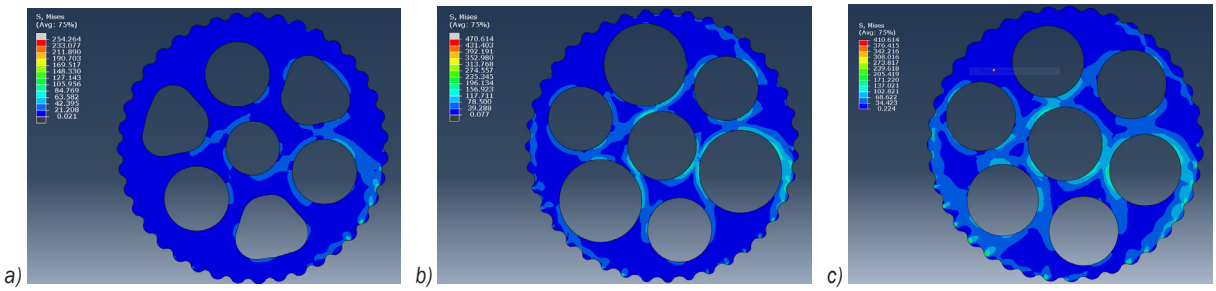

Fig. 9. *Stress analysis of three different designs: a) basic design, b) PSO, and c) QPSO*

QPSO. This reduction in size creates an opposite trend with the load distribution.

The pin-cycloid disk contact stress constraint is defined in Eq. (14). However, a constraint equation cannot be defined for the stresses except for the contact surfaces of cycloid gears. The stresses that may occur in the gear body can only be controlled by finite element analysis. For this purpose, three different geometries were modelled in the ABAQUS program with the design parameters obtained. Fig. 9 shows the stresses resulting from the finite element analysis of the Basic design, PSO and QPSO in the case of full engagement. The results obtained show that in all three designs, the maximum stresses in the cycloid gear occur at the contact points with the pin.

In order to check that the optimization algorithms are suitable for cycloidal reducers, the cycloidal disc-pin contact surface should be checked. For this purpose, a path is drawn along the gear profile. An example of a path created to examine the effect of profiles on the stresses occurring on the cycloid gear surfaces is given in Fig. 10.

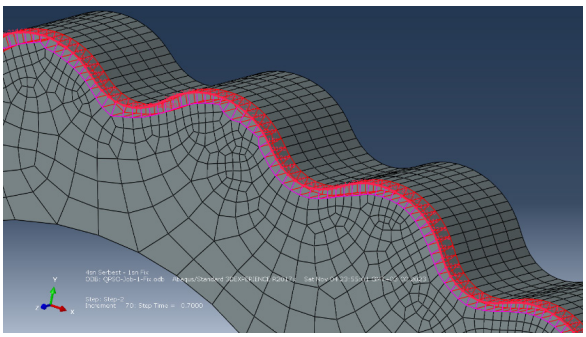

Fig. 10. *Cycloid gear path along the surface*

In Fig. 11, Von Mises stresses along the path provided in Fig. 9 under 300000 Nmm torque are presented. It has been determined that the maximum stresses are 275.76 MPa in the basic design, 371.10 MPa in PSO, and 273.04 MPa in QPSO. Considering the stresses, it is evident that the PSO geometry has the highest value. Considering the stresses on the surface and geometric features, QPSO geometry is safer than PSO.

Also, in Fig. 11 shows that the pressure does not change logarithmically along the cycloid gear, unlike the analytical solutions. This is because backlash cannot be identified in analytical solutions.

4 CONCLUSIONS

Cycloid reducers are widely used in various industrial sectors due to their ability to withstand high torque, low backlash, high positioning accuracy, resistance to wear and sudden impacts, and efficient operational performance. However, achieving their optimal design through conventional design approaches is quite challenging due to non-standard components in these reducers, particularly the cycloidal gear profile, and the direct interdependence of design parameters on each other.

In this study, two widely applied intuitive optimization algorithms, PSO and QPSO, are utilized. The primary aim is to minimize the weights and total costs of the reducer components without exceeding the safety stress limits. Proposed constraint equations are developed for weight and size optimization of a fundamental cycloidal reducer design. The results obtained from both optimization algorithms are compared with each other. The comparison of algorithm performance considers weight reduction and analytical load distribution. Subsequently, different reducers are designed using the design parameters obtained from each algorithm separately. Each resulting reducer design undergoes finite element analysis and is compared with others.

As a result, it is determined that the proposed constraint conditions and boundary values are appropriate for the weight reduction problem. Furthermore, it is established that the PSO algorithm reduces weight by 33.3 %, while the QPSO algorithm reduces it by 33.8 % compared to the basic design.

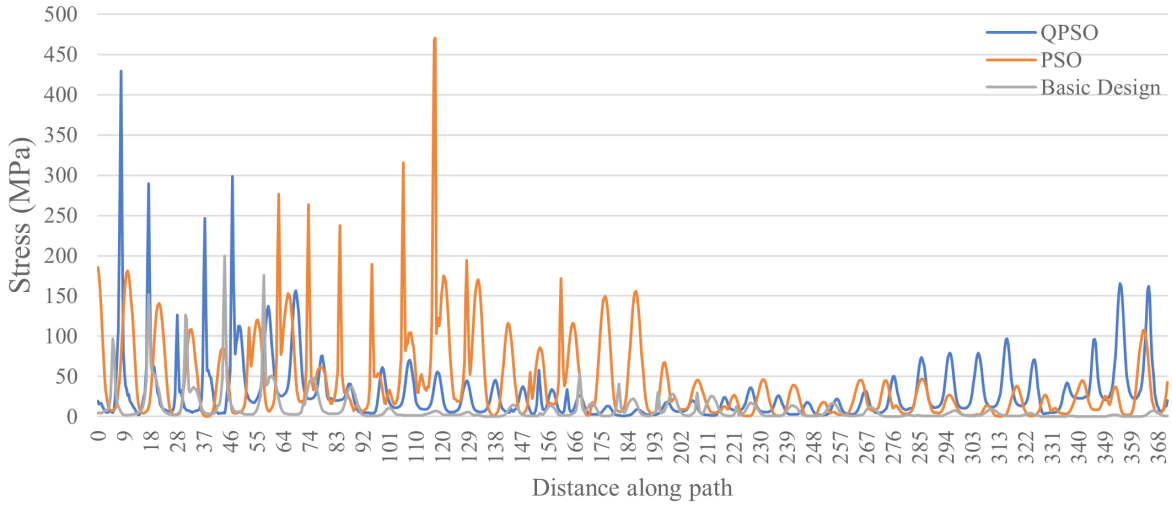

Fig. 11. *Comparison of stresses occurring along a path in cycloid gears*

Analyses reveal that maximum stresses occur at the contact surfaces between the cycloid gear and the pins. This finding validates the constraint conditions and boundary values used for defining clearances inside the cycloid gear. However, there is not yet a constraint condition defined for stresses occurring on the inner surface of the cycloid gear. For this reason, finite element analysis is currently an important verification tool for the products obtained from optimization algorithms.

In the future, further studies as a continuation of this research could explore the use of more intuitive algorithms and hybrid algorithms for enhanced optimization in this field. In addition, it is observed that the stresses in the cycloid disc body increase as the size decreases. For this reason, lifespan calculations should also be carried out in future studies.

5 REFERENCES

[1] Jiang, N., Wang, S., Xie, X., Yuan, X., Yang, A., Zhang, J. (2022) A vectorial modification methodology based on an efficient and accurate cycloid tooth profile model. *Precision Engineering*, vol. 73, p. 435-456, **DOI:10.1016/j.precisioneng.2021.10.008**.

[2] Li, T., An, X., Deng, X., Li, J., Li, Y. (2020). A new tooth profile modification method of cycloidal gears in precision reducers for robots. *Applied Sciences*, vol. 10, no. 4, p. 1266-1282, **DOI:10.3390/app10041266**.

[3] Xu, L.X., Chen, B.K. Li, C.Y. (2019). Dynamic modelling and contact analysis of bearing-cycloid-pinwheel transmission mechanisms used in joint rotate vector reducers. *Mechanism and Machine Theory*, vol. 137, p. 432-458, **DOI:10.1016/j.mechmachtheory.2019.03.035**.

[4] Yang, Y., Zhou, G., Chang, L., Chen, G. (2021). A modelling approach for kinematic equivalent mechanism and rotational transmission error of RV reducer. *Mechanism and Machine Theory*, vol. 163, 104384, **DOI:10.1016/j.mechmachtheory.2021.104384**.

[5] Li, X., Li, C., Wang, Y., Chen, B. Lim, T.C. (2017). Analysis of a cycloid speed reducer considering tooth profile modification and clearance-fit output mechanism. *Journal of Mechanical Design*, vol. 139, no. 3, **DOI:10.1115/1.4035541**.

[6] Han, L., Guo, F. (2016). Global sensitivity analysis of transmission accuracy for RV-type cycloid-pin drive. *Journal of Mechanical Science and Technology*, vol. 30, p. 1225-1231, **DOI:10.1007/s12206-016-0226-2**.

[7] Wang, H., Shi, Z.Y., Yu, B., Xu, H. (2019). Transmission performance analysis of RV reducers influenced by profile modification and load. *Applied Sciences*, vol. 9, no. 19, **DOI:10.3390/app9194099**.

[8] Korkmaz, F., Karayel, D. (2023). *A Clearances Reduction System with Pre-Stressed Tooth Contact in Cycloidal Reducers*. Turkish Patent Office, Ankara.

[9] Li, T., Xu, H., Tian, M. (2020). A loaded analysis method for rv cycloidal-pin transmission based on the minimum energy principle. *Strojniški vestnik - Journal of Mechanical Engineeing*, vol. 66, no. 11, p. 655-667, **DOI:10.5545/sv-jme.2020.6868**.

[10] Li, X., Tang, L., He, H., Sun, L. (2022). Design and load distribution analysis of the mismatched cycloid-pin gear pair in RV speed reducers. *Machines*, vol. 10, no. 8, **DOI: 10.3390/machines10080672**.

[11] Chang, L.C., Tsai, S.J., Huang, C.H. (2022). Contact characteristics of cycloid planetary gear drives considering backlashes and clearances. *Forschung im Ingenieurwesen*, vol. 86, **DOI:10.1007/s10010-021-00535-1**.

[12] Matejic, M., Blagojevic, M., Disic, A., Matejic, M., Milovanovic, V. Miletic, I. (2023). A dynamic analysis of the cycloid disc stress-strain state. *Applied Sciences*, vol. 13, no. 7, DOI: **10.3390/app13074390**.

[13] Li, Y.P., Huang, G.H., Nie, S.L. (2010). Planning water resources management systems using a fuzzy-boundary

interval-stochastic programming method. *Advances in Water Resources*, vol. 33, no. 9, p. 1105-1117, **DOI:10.1016/j.advwatres.2010.06.015.**

[14] Wang, Y., Qian, Q., Chen, G., Jin, S. Chen, Y. (2017). Multi-objective optimization design of cycloid pin gear planetary reducer. *Advances in Mechanical Engineering*, vol. 9, no. 9, **DOI:10.1177/1687814017720053**.

[15] Yang, M., Zhang, D., Cheng, C., Han, X. (2021). Reliability-based design optimization for RV reducer with experimental constraint. *Structural and Multidisciplinary Optimization*, vol. 63, p. 2047-2064, **DOI:10.1007/s00158-020-02781-3**.

[16] Zhang, Y., Li, L. Ji, S. (2022). Influence of cycloid-pin gear design parameters on bearing capacity and optimized design. *Journal of the Brazilian Society of Mechanical Sciences and Engineering*, vol. 44, 123, **DOI:10.1007/s40430-022-03426-w**.

[17] Wang, J., Luo, S., Su, D. (2016). Multi-objective optimal design of cycloid speed reducer based on genetic algorithm. *Mechanism and Machine Theory*, vol. 102, p. 135-148, **DOI:10.1016/j.mechmachtheory.2016.04.007**.

[18] Zhang, Y., Huang, J.Y., He, W. (2022). Multi-objective optimization of cycloidal gear based on segmental modification of pressure angle. *Journal of Mechanical Science and Technology*, vol. 36, p. 3535-3545, **DOI:10.1007/s12206-022-0630-8**.

[19] Huang, J., Li, C., Chen, B. (2020). Optimization design of RV reducer crankshaft bearing. *Applied Sciences*, vol. 10, no. 18, **DOI:10.3390/APP10186520**.

[20] Dereli, S., Köker, R., Öylek, İ., Ay, M. (2019). A comprehensive research on the use of swarm algorithms in the inverse kinematics solution. *Journal of Polytechnic*, vol. 22, no. 1, p. 75-79, **DOI:10.2339/politeknik.374830**.

[21] Dereli, S. (2022). A novel approach based on average swarm intelligence to improve the whale optimization algorithm. *Arabian Journal for Science and Engineering*, vol. 47, p. 1763-1776, **DOI:10.1007/s13369-021-06042-3**.

[22] Bhoskar, T., Kulkarni, O.K., Kulkarni, N.K., Patekar, S.L., Kakandikar, G.M., Nandedkar,V.M. (2015). Genetic algorithm and its applications to mechanical engineering: A review, *Materials Today Proceedings*, vol. 2, no. 4-5, p. 2624-2630, **DOI:10.1016/j.matpr.2015.07.219**.

[23] Jin, S., Cao, M., Qian, Q., Zhang, G., Wang, Y. (2023). Study on an assembly prediction method of RV reducer based on IGWO algorithm and SVR model. *Sensors*, vol. 23, no. 1, 366, **DOI:10.3390/s23010366**.

[24] Top, N., Dorterler, M., Sahin, İ. (2024). Optimization of planetary gearbox using nature inspired meta-heuristic optimizers. *Proceedings of the Institution of Mechanical Engineers, Part C: Journal of Mechanical Engineering Science*, vol. 238, no. 8, **DOI:10.1177/095440622311960**.

[25] Dereli, S., Köker, R. (2021). Strengthening the PSO algorithm with a new technique inspired by the golf game and solving the complex engineering problem. *Complex & Intelligent Systems*, vol. 7, p. 1515-1526, **DOI:10.1007/s40747-021-00292-2**.

[26] Jain, M., Saihjpal, V., Singh, N., Singh, S.B. (2022). An overview of variants and advancements of PSO algorithm. *Applied Sciences*, vol. 12, no. 17, p. 8392-8413, **DOI:10.3390/app12178392**.

[27] Flori, A., Oulhadj, H., Siarry, P. (2022). Quantum particle swarm optimization: an auto-adaptive PSO for local and global optimization. *Computational Optimization and Applications*, vol. 82, p. 525-559, **DOI:10.1007/s10589-022-00362-2**.

[28] Djemame, S., Batouche, M., Oulhadj, H., Siarry, P. (2019). Solving reverse emergence with quantum PSO application to image processing. *Soft Computing*, vol. 23, p. 6921-6935, **DOI:10.1007/s00500-018-3331-6**.

[29] Vaze, R., Deshmukh, N., Kumar, R., Saxena, A. (2021). Development and application of quantum entanglement inspired particle swarm optimization. *Knowledge-Based Systems*, vol. 219, 106859, **DOI:10.1016/j.knosys.2021.106859**.

[30] Dereli, S., Köker, R. (2018). IW-PSO approach to the inverse kinematics problem solution of a 7-DOF serial robot manipulator. *Sigma Journal of Engineering and Natural Sciences*, vol. 36, no. 1, p. 77-85.

[31] Yawei, L. Yuanzhe, W. (2012). *Design of a Cycloid Reducer*, Linnaeus University, Linnaeus.

[32] Rao, Z. (2011). Planetary transmission mechanism design. Natl. Def. Ind. Press, vol. 11.

[33] Waghole, V., , Tiwari, R. (2014). Optimization of needle roller bearing design using novel hybrid methods. *Mechanism and Machine Theory*, vol. 72, p. 71-85, **DOI:10.1016/j.mechmachtheory.2013.10.001**.

[34] Rajeswara Rao, B., Tiwari, R. (2007). Optimum design of rolling element bearings using genetic algorithms. *Mechanism and Machine Theory*, vol. 42, no. 2, p. 233-250, **DOI:10.1016/j.mechmachtheory.2006.02.004**.

[35] Qiu, J., Gong, L., Liu, L., Luo, L., J. Lou, (2023). An novel optimal design method for segmented modification of cycloid gear based on improved transmission efficiency. *Journal of Advanced Mechanical Design, Systems, and Manufacturing*, vol. 17, no. 6, p. 1-13, **DOI:10.1299/jamdsm.2023jamdsm0069**.

[36] Brnic, J., Turkalj, G., Lanc, D., Canadija, M., Brcic, M., Vukelic, G. (2014). Comparison of material properties: Steel 20MnCr5 and similar steels. *Journal of Constructional Steel Research*, vol. 95, p. 81-89, **DOI:10.1016/j.jcsr.2013.11.024**.

[37] Hu, Y., Li, G., Zhu, W., Cui, J. (2020). An elastic transmission error compensation method for rotary vector speed reducers based on error sensitivity analysis. *Applied Sciences*, vol. 10, no. 2, **DOI:10.3390/app10020481**.